Investigating the efficacy of triple artemisinin-based combination therapies (TACTs) for treating *Plasmodium falciparum* malaria patients using mathematical modelling

Saber Dini,[a] Sophie Zaloumis,[a] Pengxing Cao,[b] Ric N Price,[c,d] Freya J.I. Fowkes,[a,e,f] James M McCaw,[a,b,g,h] Julie A Simpson[a,#]

[a] Centre for Epidemiology and Biostatistics, Melbourne School of Population and Global Health, University of Melbourne, Melbourne, Australia

[b] School of Mathematics and Statistics, University of Melbourne, Melbourne, Australia

[c] Global and Tropical Health Division, Menzies School of Health Research and Charles Darwin University

[d] Centre for Tropical Medicine and Global Health, Nuffield Department of Clinical Medicine, University of Oxford

[e] Burnet Institute, Disease Elimination Program, Public Health, Melbourne, Australia

[f] Department of Epidemiology and Preventative Medicine and Department of Infectious Diseases, Monash University, Melbourne, Australia

[g] Peter Doherty Institute for Infection and Immunity, The Royal Melbourne Hospital and University of Melbourne, Melbourne, Australia

[h] Murdoch Children's Research Institute, The Royal Children's Hospital, Melbourne, Australia

Running Head: Mathematical Modelling of TACT

#Address correspondence to Julie A. Simpson, julieas@unimelb.edu.au.

Abstract

The first line treatment for uncomplicated falciparum malaria is artemisinin-based combination therapy (ACT), which consists of an artemisinin derivative co-administered with a longer acting partner drug. However, the spread of *Plasmodium falciparum* resistant to both artemisinin and its partner drugs poses a major global threat to malaria control activities. Novel strategies are needed to retard and reverse the spread of these resistant parasites. One such strategy is triple artemisinin-based combination therapy (TACT). We developed a mechanistic within-host mathematical model to investigate the efficacy of a TACT (dihydroartemisinin-piperaquine-mefloquine - DHA-PQ-MQ), for use in South-East Asia, where DHA and PQ resistance are now increasingly prevalent. Comprehensive model simulations were used to explore the degree to which the underlying resistance influences the parasitological outcomes. The effect of MQ dosing on the efficacy of TACT was quantified at varying degrees of DHA and PQ resistance. To incorporate interactions between drugs, a novel model is presented for the combined effect of DHA-PQ-MQ, which illustrates how the interactions can influence treatment efficacy. When combined with a standard regimen of DHA and PQ, the administration of three 8.3 mg/kg doses of MQ was sufficient to achieve parasitological efficacy greater than that currently recommended by WHO guidelines.

Introduction

Over the last decade, significant gains have been made towards the control and elimination of malaria. Despite this progress, almost half a billion people still die from malaria

each year. Disturbingly, in 2016 there were five million more cases of malaria than the previous year (2017 WHO report (1)), emphasising the fragile nature of malaria control. Early diagnosis and treatment with highly effective antimalarial drug regimens remains central to all national malaria control activities. Artemisinin-based combination therapies (ACTs) are the first line therapy in almost all malaria endemic countries, due to their high efficacy, tolerability and ability to reduce ongoing transmission of the parasite. ACTs are comprised of two components: an artemisinin derivative and a partner drug. The artemisinin derivative has a high antimalarial potency, killing a large proportion of parasites, however, these compounds are rapidly eliminated, leaving a residual parasite population that, if left untreated, will likely recrudesce. A slowly eliminated, partner drug, is required to provide a sustained antimalarial activity, capable of killing the remaining parasites (2).

ACTs have remained highly efficacious for almost two decades, but are now under threat from the emergence of drug resistant parasites (2, 3). In 2009, a high proportion of patients with markedly delayed parasite clearance were reported from the western region of Cambodia, and this was confirmed as being attributable to artemisinin resistance (3). These parasites have now spread across the Greater Mekong Region (4, 5). Delayed parasite clearance and higher gametocyte carriage, due to the artemisinin derivative resistance, drive selection of resistance to the partner drug (6), and in South-East Asia, this has resulted in declining efficacy of all the ACTs currently recommended by WHO (7). In some parts of the Greater Mekong Region, the spread of highly drug resistant parasites poses a major threat to malaria control activities. The emergence of an untreatable *P. falciparum* will result in an inevitable rise in malaria incidence, epidemics and associated

66 morbidity and mortality.

67 The development of alternative strategies is crucial to ensuring the ongoing success
68 of malaria control efforts. Triple Artemisinin-based Combination Therapy (TACT) is
69 a novel strategy by which a new partner drug is added to an established ACT. TACT
70 has the potential to prevent the emergence of a *de novo* resistance as well as rescuing a
71 regimen in which one of the ACT components is already failing. Two antimalarial clinical
72 trials are underway to determine the efficacy of TACT for uncomplicated falciparum
73 malaria: Artemether-Lumefantrine plus Amodiaquine (AL-AQ) and Dihydroartemisinin-
74 Piperaquine plus Mefloquine (DHA-PQ-MQ). These are being compared to the standard
75 ACTs (AL and DHA-PQ) alone (see trial number NCT02453308 in clinicaltrials.gov).

76 In this work, we developed a within-host mathematical model (8) to explore the
77 efficacy of TACTs, with a particular focus on DHA-PQ-MQ, since DHA-PQ is widely
78 administered in South-East Asia, and is currently associated with very high failure rates
79 in some regions (9, 10, 11). The model accommodates a high level of biological details,
80 such as drug-drug interaction (12, 13), stage-specificity of parasite killing (14, 15, 16,
81 17) and between-patient and between-isolate variability (17). We used the model to
82 simulate different levels of resistance and quantify the degree to which this compromises
83 the efficacy of TACT. The optimal MQ dosing regimen was determined for various degrees
84 of resistance to DHA-PQ.

Results

Simulated drug concentrations and parasite burden are shown in Fig. 1. The median concentration of the drugs (lines) along with the between-subject variabilities (the shaded regions show the area between the 2.5% and 97.5% percentiles) are presented in Fig. 1a, and the parasitaemia of 100 randomly selected patients in Fig. 1b. Fig. 1c presents the Kaplan-Meier estimation of the probability of cure, along with the 95% confidence intervals illustrated by the shaded region.

Parasite resistance to antimalarial drugs can manifest in a couple of different ways that affect the killing profile of a drug (see the concentration-effect curves in Fig. 2 (18)). These include i) increasing EC_{50} (the red curve), ii) reducing the size of the killing window in the intra-erythrocytic parasite life-cycle, and iii) decreasing γ and/or E_{max} (the blue curve). The degree of resistance was modelled initially by varying EC_{50} of PQ, in scenarios where the parasites are sensitive or resistant to DHA. The influence of other manifestations of resistance on TACT efficacy are outlined in Supplementary Material 1.

The level of resistance and the resultant risk of treatment failure varies with geographical region. Table 1 demonstrates a large variation in DHA-PQ efficacy in different regions across South-East Asia (19). The risk of failures in Aoral and Chi Kraeng in Cambodia are 51.9% and 62.5% treatment failures, respectively, whereas in Siem Pang it is only 8.3%. Similar large variations in the probability of treatment failure are observed in Vietnam. According to the WHO treatment guidelines, when the risk of failure exceeds 10%, a treatment is considered suboptimal, and steps should be taken to change the policy to a more efficacious antimalarial regimen.

Sensitivity to DHA

In the first investigated scenario, the parasites were assumed sensitive to DHA (sampling interval of $EC_{50,D}$ was limited to $(0, 10]$ ng/ml), and resistance level to PQ was varied. Fig. 3a shows how the probability of cure at day 42 of follow-up varies with EC_{50} of PQ over the deciles of $(11, 94]$ ng/ml. The top labels in this figure show the geographical regions in South-East Asia (Table 1) that have observed DHA-PQ day 42 cure rates equal to the corresponding simulated values (19).

The probability of cure declines as EC_{50} of PQ increases. Without MQ, the probability of cure with DHA-PQ is below 90%, over $EC_{50,P} \in (36, 94]$, which includes Binh Phuoc and Bu Gia Map. This scenario was unable to produce the probabilities of cure observed in all of the geographical regions, shown in Table 1.

The addition of a single 8.3 mg/kg dose of MQ on day 3 significantly raised the probability of cure. Day 3 administration of MQ was chosen, since at this time patients are clinically better, the drug is better tolerated and bioavailability is higher (20). The improvement in efficacy with a single dose of MQ was insufficient to ensure successful treatment in Bu Gia Map. In this region, a second dose at day 2 was required. When the parasites are sensitive to DHA, but resistant to PQ, two doses of MQ on days 2 and 3 were sufficient to achieve cure in all locations. Administration of three doses of MQ did not provide significant benefit over a two dose MQ regimen, although might be used to guarantee the success of the TACT.

Resistance to DHA

Concurrent resistance to DHA and PQ is now documented in Cambodia and Vietnam (9). To simulate a high level of DHA resistance, we set $EC_{50,D} \in (50, 100]$ ng/ml, and varied the intensity of resistance to PQ, $EC_{50,P} \in (11, 94]$ ng/ml. Using the same dosing regimens as those in Fig. 3a, resistance to DHA leads to a significant decline in the efficacy of DHA-PQ, as shown in Fig. 3b. When combined with a single 8.3 mg/kg dose of MQ, the efficacy of the TACT was improved significantly, but except for Siem Pang, it was clearly not sufficient.

Administration of MQ on days 2 and 3 provided sufficient efficacy in Binh Phuoc and Bu Gia Map, but was still insufficient for Aoral and Chi Kraeng. An additional dose of MQ was needed on day 1 to obtain a successful treatment in all of the regions. Note that administering 8.3 mg/kg of MQ over three days (25 mg/kg in total) is currently the recommended dosing regimen by WHO for the ACT of MQ plus artesunate (18).

The influence of the antagonistic PQ-MQ interaction

The effect of the PQ-MQ interaction parameter, α, on the probability of cure was then investigated. Fig. 4a shows the combined killing effect of the drugs, E, over time for a selected patient with two different values of the interaction parameter: $\alpha = 3.3$ (antagonism) and $\alpha = 1$ (zero-interaction); the other parameters were kept constant. The killing effect for $\alpha = 1$ (solid line) is significantly higher than that for $\alpha = 3.3$ (dashed line), indicating the extent to which the drugs can nullify each other's effect, and the loss in the overall efficacy of TACT.

148 The effect of the interaction parameter, α, on the efficacy was further assessed by
149 restricting the resistance level to that corresponding to Chi Kraeng ($EC_{50,P} \in (69, 78]$)
150 and estimating the probability of cure for different values of α; DHA resistance is also
151 assumed. The results demonstrated a significant difference between the probabilities of
152 cure at different values of α; Fig. 4b. For example, when $\alpha < 1$ (synergism), one dose
153 of MQ was enough to provide 90% efficacy. In contrast, when $\alpha > 1$ (antagonism) the
154 probability of cure fell well below 90%. Similarly, the probability of cure declined with
155 increasing α (*i.e.* antagonism intensification) for MQ administration on days 2 and 3
156 and on days 1, 2 and 3. Of note, the three 8.3 mg/kg doses of MQ achieved greater
157 than 90% efficacy at all values of α, even at levels indicative of very strong antagonism.
158 This highlights the robustness of this dosing regimen in producing a successful treatment.
159 The antagonism between PQ and MQ had an important impact on the efficacy of the
160 TACT, and neglecting this may result in an underestimation of the dose of MQ required
161 for successful treatment across different regions.

162 The effect of other manifestations of resistance on the efficacy of the TACT are il-
163 lustrated in Supplementary Material 1. Fig. S1 presents the probability of survival at
164 different levels of resistance produced by varying maximum killing effect of PQ, $E_{max,P}$.
165 Similar to the case where EC_{50} was the manifestation of resistance, shown in Fig. 3, the
166 results indicate that the three 8.3 mg/kg doses of MQ are sufficient to provide the desir-
167 able probability of cure at every level of resistance. The outcomes were consistent when
168 the killing window of PQ was shortened, as shown in Fig. S2. However, the probability
169 of cure became extremely low, when resistance was high. Nevertheless, three 8.3 mg/kg
170 doses of MQ overcame high levels of resistance and ensured high probability of cure.

Discussion

We have presented a novel mathematical model to investigate the efficacy of different regimens for triple artemisinin combination therapies (TACTs). Our analysis focused on DHA-PQ-MQ, since DHA-PQ is a widely used ACT in South-East Asia with declining efficacy in several locations (9, 10, 11). The addition of MQ to DHA-PQ has potential to improve treatment, since the ACT of artesunate-MQ retains high efficacy, following its reintroduction as a first-line treatment in Cambodia (7). Our results suggest that a single dose of MQ can improve the treatment efficacy of DHA-PQ significantly, and would be an appropriate regimen for regions such as Siem Pang in Cambodia and Binh Phuoc in Viet Nam. However, it is likely to be insufficient in regions where there is pre-existing high grade resistance to PQ, such as Bu Gia Map in Viet Nam and Aoral and Chi Kraeng in Cambodia. The addition of two doses of MQ would be beneficial, but efficacy would still be compromised in the regions where there was high level of resistance to both PQ and DHA, such as Chi Kraeng. To achieve a cure rate of greater than 90%, as recommended by the WHO, three doses of MQ (8.3 mg/kg) need to be administered in conjunction with the standard three days regimen of DHA-PQ. Such a dose of MQ, has already been shown to be well tolerated and safe, and is recommended in the WHO treatment guidelines (18).

Our model enabled us to simulate the PK and PD following TACT administration to patients with malaria, and provided important insights into the way in which the underlying mechanisms of drug action affect treatment efficacy. By taking account of between-patient and between-isolate variability, we were able to explore treatment efficacy

across a wide range of different scenarios reflecting varying parasite resistance to the different drug components. The results showed similar trends for different resistance manifestations, confirming the robustness of the proposed dosing regimen of DHA-PQ-MQ.

We have proposed a novel empirical model to accommodate the effect of the combined drugs, assuming that PQ and MQ (both quinoline compounds) have similar modes of action, which differs from that of DHA (an endoperoxide compound). The killing effects of PQ-MQ and DHA were therefore assumed to be independent. This justified using a combination of Bliss independence and Loewe additivity to define the combined effect of the whole compound (see Eqn. (1)).

To facilitate the dissemination of our model and assist clinical researchers to investigate how different PK and PD parameters and dosing schemes influence parasitological outcomes, we have produced an online application that allows varying the values of parameters and simulating the model: appTACT. By predicting the fate of malaria infection in patients, the online application can provide a means for *e.g.* estimating the required sample size of an antimalarial clinical efficacy study.

Our mathematical model can be used to guide the development of suitable TACT regimens for investigation in clinical trials. Determining dosing regimens that are robust to a wide range of scenarios helps rationalize the logistical and financial challenges of phase 2 and 3 clinical trials. Further improvements in the model can be made to increase its fidelity to the underlying biology. For instance, by consideration of the artemisinins PK (e.g. bioavailability) dependence on parasite density (21) and different bioavailability

of MQ at different administered days (20). The PD model can also be improved by incorporating more complexities underlying drug action, such as the dependence of killing effect on the timespan parasites are exposed to drugs (22, 23, 24, 25). However, in this initial analysis, we aimed to focus on the generality of the model and leave these modifications for future studies. Although we did not explore the degree to which the efficacy of TACT influenced other aspects of malaria control, such as the transmissibility of the parasite, this certainly warrants further investigation, since a more comprehensive perspective will be needed on the suitability of deploying TACT in areas of high drug resistance.

Materials and Methods

Mathematical Model

The pharmacokinetic-pharmacodynamic (PK-PD) model presented in Zaloumis et al. 2012 (17) was used to model the dynamics of drug concentrations and parasite burden within an individual. In brief, this model describes the time-evolution of the number of parasites in the body, N, by the following difference equations:

$$N(a,t) = \begin{cases} N(a-1,t-1)\left(1-E(a-1,t-1)\right), & 1 < a \leq 48, \\ N(48,t-1)\left(1-E(48,t-1)\right) \times \text{PMF}, & a = 1, \end{cases}$$

where a is the parasites' age, taking only integer values over [1 48], t is time and PMF is the parasite multiplication factor, which represents the number of merozoites released

into blood by a shizont at the end of its lifecycle. $E(a,t)$ is the combined killing effect of the drugs, and has been modified from that presented in Zaloumis et al. 2012 to account for three drugs and accommodate drug interactions. The combined killing effect of the drugs is between 0 and 1, and dependent upon the age of parasites during $[t, t+1)$. The number of detectable parasites circulating in the blood, $M(t)$, is determined by

$$M(t) = \sum_{a=1}^{48} N(a,t)g(a),$$

where $g(a)$ accounts for the reduction in the number of circulating parasites in the blood due to sequestration, estimated to be

$$g(a) = \begin{cases} 1, & a < 11, \\ 2^{\frac{11-a}{3}}, & a \geq 11, \end{cases}$$

where we assumed sequestration begins at age 11 and intensifies with age (16, 26). In the ensuing section, we explain the details of modelling the combined effect of the drugs, E.

The PK models for the three drugs considered, DHA, PQ and MQ, are well characterized; one-compartment models were used for DHA and MQ and a two-compartment model for PQ (27, 28, 29). The PK parameter values are drawn from the literature and provided in Table 2.

Combined killing effect of the drugs

The combined killing effect of the drugs is modulated by the manner in which they interact with each other. Synergistic interaction between drugs produces a stronger combined

effect compared to the case where they do not interact, *i.e.* zero-interaction (also known as pure additivity). Conversely, antagonistic drug-drug interactions can nullify their additive effect, and produce a lower combined effect than that for the zero-interaction case. Therefore, to model the combined effect, E, we must first identify how the drugs interact.

An empirical approach was taken, modelling zero-interaction as the reference (null) model (30, 31, 32), since the mechanisms underlying the killing effects are complex and not completely understood (33). Among the existing empirical approaches of modelling zero-interaction, two are more prominent and widely used: *Loewe additivity* (34) and *Bliss independence* (35). Loewe additivity is suggested to be a suitable concept for zero-interaction when non-interacting drugs have similar modes of action, however, when the drugs are believed to act independently, Bliss independence is more appropriate (31, 32).

It has been suggested that MQ and PQ kill parasites through a similar mechanism, involving the disruption of haem detoxification in the parasite vacuole (33, 36, 37). DHA has a different mode of action, which involves the generation of free radicals and reactive intermediates that target various proteins of parasites (36, 38, 39). The PK and PD interactions of DHA with PQ and MQ appear to be negligible (13).

The independent mechanisms of action of DHA and PQ-MQ justifies using the Bliss independence concept for modelling the combined killing effect, E, given by

$$E = E_D + E_{PM} - E_D E_{PM}, \tag{1}$$

where E_D is the killing effect of DHA and E_{PM} is the combined effect of PQ and MQ.

268 We assume Michaelis-Menten kinetics for E_D:

$$E_D = E_{max,D}\frac{C_D^{\gamma_D}}{C_D^{\gamma_D} + EC_{50,D}^{\gamma_D}}\mathbf{1}_{W_D}(a),$$

269 where $E_{max,D}$ is the maximum killing effect of DHA; C_D is DHA concentration; $EC_{50,D}$
270 is the concentration at which 50% of the maximum killing effect is obtained; γ_D is the
271 sigmoidicity (also known as slope) of the concentration-effect curve; $\mathbf{1}_W(a)$ is an indicator
272 function, used to implement the age-specific killing of drugs, defined by

$$\mathbf{1}_W(a) = \begin{cases} 1, & a \in W, \\ 0, & \text{otherwise}, \end{cases}$$

273 where W is the age window (interval) where the antimalarial drugs are able to kill the
274 parasites; W_D is the killing window of DHA.

275 To define E_{PM}, models incorporating the Loewe additivity concept (as PQ and MQ
276 have similar modes of action) were used, which include only one parameter for the effect
277 of the interaction between PQ and MQ (31, 32, 40). These models are more specified
278 to the framework of drug interaction, in contrast to the statistical models that usually
279 have multiple parameters (41, 42, 43). A detailed description of the examined models is
280 provided in Supplementary Material 2. The final model selected was a combination of
281 the models described in Tallarida 2006 (32) and Machado, Robinson 1994 (40):

$$E_{PM} = E_{max,P}\frac{C_{PM}^{\gamma_P}}{C_{PM}^{\gamma_P} + EC_{50,P}^{\gamma_P}},$$

where

$$C_{PM} = \left(C_P^{\alpha}\ \mathbf{1}_{W_P}(a) + C_{eq,M}^{\alpha}\ \mathbf{1}_{W_M}(a)\right)^{\frac{1}{\alpha}}, \tag{2}$$

and

$$C_{eq,M} = E_P^{-1}\left(E_M(C_M)\right),$$

where E_M is the killing effect of MQ and E_P^{-1} is the inverse of the killing effect of PQ, given by

$$E_P^{-1}(x) = EC_{50,P}\left(\frac{x}{E_{max,P} - x}\right)^{\frac{1}{\gamma_P}},$$

where $E_{max,P}$ and $EC_{50,P}$ are the maximum killing effect of PQ and the concentration at which half of the maximum killing effect is produced, respectively; W_P and W_M are the killing windows of PQ and MQ, respectively. Zero-interaction is produced by Eqn. (2) when $\alpha = 1$; the values of $1 < \alpha < \infty$ and $0 < \alpha < 1$ produce antagonism and synergism, respectively. Note that PQ is considered to be more potent than MQ; see Supplementary Material 2 for further information.

Isobolograms, widely used in pharmacology and toxicology studies, can inform on the nature of drug-drug interactions. These present data on the parasiticidal effect of paired drug concentrations. The combination of drug concentrations is then compared with the zero-interaction isobole (also known as linear isobole) (44); see Fig. 5a. When the pairs of drugs concentrations are close to the linear isobole, zero-interaction is inferred, and when they lie significantly above or below the linear isobole, antagonism or synergism can be inferred, respectively.

Using this approach, Davis et al. 2006 (13) showed that the paired PQ and MQ data

were significantly above the zero-interaction isobole (dashed line), indicating a strong antagonistic interaction between PQ and MQ; Fig. 5a. The combined killing effect of PQ-MQ, E_{PM}, was fitted to this data, and PQ-MQ interaction parameter was estimated to be $\alpha = 3.3$. Fig. 5b shows predicted E_{PM} for $\alpha = 3.3$ for varying PQ and MQ concentrations. The killing effects of DHA and PQ-MQ were applied to Eqn. (1) to estimate the combined effect of DHA-PQ-MQ and simulate the PD model; see Supplementary Material 2 for further details.

Model simulation

Latin Hypercube Sampling (LHS) was used to efficiently sample the parameter space (45), and simulate the PK profiles and parasitological responses. The distributions of the parameter values of the PK and PD models are presented in Tables 2 and 3, respectively. A triangular distribution was used for generating samples of α, with a peak at $\alpha = 3.3$, estimated by fitting the model to the data, as explained in the previous section. The lower and upper bounds were selected to be 1 (zero-interaction) and 16 (very strong antagonism), respectively. The initial parasite burden was assumed to have a log-normal distribution with a geometric mean of 1.14×10^{11} and standard deviation of 1.13 on the log-scale; Table 3.

The probability of cure (*i.e.* 1 - probability of failure) was used as a measure of drug efficacy, and Kaplan-Meier survival analysis was carried out on the simulated parasite versus time profiles of the patients, to estimate the probabilities of cure at day 42 of follow-up. Treatment failure was defined as parasite recrudescence, in which the peripheral

parasitaemia exceeded the microscopic limit of detection (50 parasite per μL or a total parasite biomass of 2.5×10^8).

Dosing regimens recommended by WHO were used in the simulations. These included 18.0 mg/kg/day of PQ and 4.0 mg/kg/day of DHA for three days. Current guidelines recommend a total dose of 25 mg/kg MQ in combination with 4mg/kg/day of artesunate (18). Splitting the dose of MQ (8.3 mg/kg/day for three days) improves the bioavailability of MQ, is better tolerated and and has a greater efficacy (46). Higher daily doses of MQ are associated with significant side-effects (47), and thus modelling explored the minimum dosage of MQ that results in optimal efficacy. Hence, the number of days in which a 8.3 mg/kg dose of MQ was administered was varied and the corresponding TACT efficacy was estimated.

To simulate different degrees of PQ and DHA resistance, EC_{50}, E_{max} and W were varied over the limited sampling intervals of the range of values given in Table 3. Different scenarios were considered, simulating resistance to DHA and/or PQ.

Acknowledgments

This work was supported by the NHMRC Centres for Research Excellence in Malaria Elimination (1134989) and Infectious Diseases Modelling to Inform Public Health Policy (1078068), an NHMRC Project Grant (1100394) and an ARC Discovery Project (DP170103076). FJIF was supported by Australian Research Council Future Fellowship. RNP is a Wellcome Trust Senior Fellow in Clinical Science (200909), and JAS is a NHMRC Senior Research Fellow (1104975).

References

1. WHO. 2017. World Malaria Report. World Health Organisation. URL: http://www.who.int/malaria/publications/world-malaria-report-2017/en/.

2. Fairhurst RM, Dondorp AM. 2016. Artemisinin-resistant *Plasmodium falciparum* malaria. Microbiol Spectr 4.

3. Dondorp AM, Nosten F, Yi P, Das D, Phyo AP, Tarning J, Lwin KM, Ariey F, Hanpithakpong W, Lee SJ, Ringwald P, Silamut K, Imwong M, Chotivanich K, Lim P, Herdman T, An SS, Yeung S, Singhasivanon P, Day NPJ, Lindegardh N, Socheat D, White NJ. 2009. Artemisinin resistance in *Plasmodium falciparum* malaria. N Engl J Med 361:455–467.

4. Ashley EA, Dhorda M, Fairhurst RM, Amaratunga C, Lim P, Suon S, Sreng S, Anderson JM, Mao S, Sam B, Sopha C, Chuor CM, Nguon C, Sovannaroth S, Pukrittayakamee S, Jittamala P, Chotivanich K, Chutasmit K, Suchatsoonthorn C, Runcharoen R, Hien TT, Thuy-Nhien NT, Thanh NV, Phu NH, Htut Y, Han KT, Aye KH, Mokuolu OA, Olaosebikan RR, Folaranmi OO, Mayxay M, Khanthavong M, Hongvanthong B, Newton PN, Onyamboko MA, Fanello CI, Tshefu AK, Mishra N, Valecha N, Phyo AP, Nosten F, Yi P, Tripura R, Borrmann S, Bashraheil M, Peshu J, Faiz MA, Ghose A, Hossain MA, Samad R, Rahman MR, Hasan MM, Islam A, Miotto O, Amato R, MacInnis B, Stalker J, Kwiatkowski DP, Bozdech Z, Jeeyapant A, Cheah PY, Sakulthaew T, Chalk J, Intharabut B, Silamut K, Lee SJ, Vihokhern B, Kunasol C, Imwong M, Tarning J, Taylor WJ, Yeung S, Woodrow CJ, Flegg JA, Das D, Smith J, Venkatesan M, Plowe CV, Stepniewska K, Guerin

PJ, Dondorp AM, Day NP, White NJ. 2014. Spread of artemisinin resistance in *Plasmodium falciparum* malaria. N Engl J Med 371:411–423.

5. Tun KM, Imwong M, Lwin KM, Win AA, Hlaing TM, Hlaing T, Lin K, Kyaw MP, Plewes K, Faiz MA, Dhorda M, Cheah PY, Pukrittayakamee S, Ashley EA, Anderson TJC, Nair S, McDew-White M, Flegg JA, Grist EPM, Guerin P, Maude RJ, Smithuis F, Dondorp AM, Day NPJ, Nosten F, White NJ, Woodrow CJ. 2015. Spread of artemisinin-resistant *Plasmodium falciparum* in Myanmar: a cross-sectional survey of the K13 molecular marker. Lancet Infect Dis 15:415–421.

6. Amato R, Lim P, Miotto O, Amaratunga C, Dek D, Pearson RD, Almagro-Garcia J, Neal AT, Sreng S, Suon S, Drury E, Jyothi D, Stalker J, Kwiatkowski DP, Fairhurst RM. 2017. Genetic markers associated with dihydroartemisinin-piperaquine failure in *Plasmodium falciparum* malaria in Cambodia: a genotype-phenotype association study. Lancet Infect Dis 17:164–173.

7. WHO. 2017. Artemisinin and artemisinin-based combination therapy resistance. World Health Organization. URL: www.who.int/malaria/publications/atoz/artemisinin-resistance-april2017/en/.

8. Simpson JA, Zaloumis S, DeLivera AM, Price RN, McCaw JM. 2014. Making the most of clinical data: reviewing the role of pharmacokinetic-pharmacodynamic models of anti-malarial drugs. AAPS J 16:962–974.

9. Amaratunga C, Lim P, Suon S, Sreng S, Mao S, Sopha C, Sam B, Dek D, Try V, Amato R, Blessborn D, Song L, Tullo GS, Fay MP, Anderson JM, Tarning J, Fairhurst RM. 2016. Dihydroartemisinin-piperaquine resistance in *Plasmodium*

falciparum malaria in Cambodia: a multisite prospective cohort study. Lancet Infect Dis 16:357–365.

10. Leang R, Taylor WRJ, Bouth DM, Song L, Tarning J, Char MC, Kim S, Witkowski B, Duru V, Domergue A, Khim N, Ringwald P, Menard D. 2015. Evidence of *Plasmodium falciparum* malaria multidrug resistance to artemisinin and piperaquine in western Cambodia: dihydroartemisinin-piperaquine open-label multicenter clinical assessment. Antimicrob Agents Chemother 59:4719–4726.

11. Phuc BQ, Rasmussen C, Duong TT, Dong LT, Loi MA, Ménard D, Tarning J, Bustos D, Ringwald P, Galappaththy GL, Thieu NQ. 2017. Treatment failure of dihydroartemisinin/piperaquine for *Plasmodium falciparum* malaria, Vietnam. Emerg Infect Dis 23:715–717.

12. Ariens EJ, Simonis AM. 1964. A molecular basis for drug action*. J Pharm Pharmacol 16:137–157.

13. Davis TME, Hamzah J, Ilett KF, Karunajeewa HA, Reeder JC, Batty KT, Hackett S, Barrett PHR. 2006. *In vitro* interactions between piperaquine, dihydroartemisinin, and other conventional and novel antimalarial drugs. Antimicrob Agents Chemother 50:2883–2885.

14. Hodel EM, Kay K, Hastings IM. 2016. Incorporating stage-specific drug action into pharmacological modeling of antimalarial drug treatment. Antimicrob Agents Chemother 60:2747–56.

15. Hoshen MB, Na-Bangchang K, Stein WD, Ginsburg H. 2000. Mathematical modelling of the chemotherapy of *Plasmodium falciparum* malaria with artesunate: pos-

tulation of 'dormancy', a partial cytostatic effect of the drug, and its implication for treatment regimens. Parasitology 121:237–246.

16. Saralamba S, Pan-Ngum W, Maude RJ, Lee SJ, Tarning J, Lindegårdh N, Chotivanich K, Nosten F, Day NPJ, Socheat D, White NJ, Dondorp AM, White LJ. 2011. Intrahost modeling of artemisinin resistance in *Plasmodium falciparum*. Proc Natl Acad Sci 108:397–402.

17. Zaloumis S, Humberstone A, Charman SA, Price RN, Moehrle J, Gamo-Benito J, McCaw J, Jamsen KM, Smith K, Simpson JA. 2012. Assessing the utility of an anti-malarial pharmacokinetic-pharmacodynamic model for aiding drug clinical development. Malar J 11:303.

18. WHO. 2015. Guidelines for the treatment of malaria. World Health Organization. URL: http://www.who.int/malaria/publications/atoz/9789241549127/en/.

19. WHO. 2018. WHO malaria threats map: tracking biological challenges to malaria control and elimination. URL: http://apps.who.int/malaria/maps/threats/.

20. Price RN, Simpson JA, Teja-Isavatharm P, Than MM, Luxemburger C, Heppner DG, Chongsuphajaisiddhi T, Nosten F, White NJ. 1999. Pharmacokinetics of mefloquine combined with artesunate in children with acute falciparum malaria. Antimicrob Agents Chemother 43:341–346.

21. Lohy Das J, Dondorp AM, Nosten F, Phyo AP, Hanpithakpong W, Ringwald P, Lim P, White NJ, Karlsson MO, Bergstrand M, Tarning J. 2017. Population pharmacokinetic and pharmacodynamic modeling of artemisinin resistance in Southeast Asia. AAPS J 19:1842–1854.

22. Klonis N, Xie SC, McCaw JM, Crespo-Ortiz MP, Zaloumis SG, Simpson JA, Tilley L. 2013. Altered temporal response of malaria parasites determines differential sensitivity to artemisinin. Proc Natl Acad Sci 110:5157–62.

23. Dogovski C, Xie SC, Burgio G, Bridgford J, Mok S, McCaw JM, Chotivanich K, Kenny S, Gnädig N, Straimer J, Bozdech Z, Fidock DA, Simpson JA, Dondorp AM, Foote S, Klonis N, Tilley L. 2015. Targeting the cell stress response of plasmodium falciparum to overcome artemisinin resistance. PLOS Biol 13:e1002132.

24. Cao P, Klonis N, Zaloumis S, Dogovski C, Xie SC, Saralamba S, White LJ, Fowkes FJI, Tilley L, Simpson JA, McCaw JM. 2017. A dynamic stress model explains the delayed drug effect in artemisinin treatment of *Plasmodium falciparum*. Antimicrob Agents Chemother 61:e00618–17.

25. Cao P, Klonis N, Zaloumis S, Khoury DS, Cromer D, Davenport MP, Tilley L, Simpson JA, McCaw JM. 2017. A mechanistic model quantifies artemisinin-induced parasite growth retardation in blood-stage *Plasmodium falciparum* infection. J Theor Biol 430:117–127.

26. Udomsangpetch R, Pipitaporn B, Silamut K, Pinches R, Kyes S, Looareesuwan S, Newbold C, White NJ. 2002. Febrile temperatures induce cytoadherence of ring-stage *Plasmodium falciparum*-infected erythrocytes. Proc Natl Acad Sci 99:11825–11829.

27. Ashley EA, Stepniewska K, Lindegårdh N, McGready R, Hutagalung R, Hae R, Singhasivanon P, White NJ, Nosten F. 2006. Population pharmacokinetic assessment of a new regimen of mefloquine used in combination treatment of uncomplicated falciparum malaria. Antimicrob Agents Chemother 50:2281–5.

28. Jamsen KM, Duffull SB, Tarning J, Lindegardh N, White NJ, Simpson JA. 2011. Optimal designs for population pharmacokinetic studies of oral artesunate in patients with uncomplicated falciparum malaria. Malar J 10:181.

29. Tarning J, Ashley EA, Lindegardh N, Stepniewska K, Phaiphun L, Day NPJ, McGready R, Ashton M, Nosten F, White NJ. 2008. Population pharmacokinetics of piperaquine after two different treatment regimens with dihydroartemisinin-piperaquine in patients with *Plasmodium falciparum* malaria in Thailand. Antimicrob Agents Chemother 52:1052–1061.

30. Chou TC. 2006. Theoretical basis, experimental design, and computerized simulation of synergism and antagonism in drug combination studies. Pharmacol Rev 58:621–681.

31. Greco WR, Bravo G, Parsons JC. 1995. The search for synergy: a critical review from a response surface perspective. Pharmacol Rev 47.

32. Tallarida RJ. 2006. An overview of drug combination analysis with isobolograms. J Pharmacol Exp Ther 319.

33. Horn D, Duraisingh MT. 2014. Antiparasitic chemotherapy: from genomes to mechanisms. Annu Rev Pharmacol Toxicol 54:71–94.

34. Loewe S. 1928. Die quantitativen probleme der pharmakologie. Ergebnisse der Physiol 27:47–187.

35. Bliss CI. 1939. The toxicity of poisons applied jointly. Ann Appl Biol 26:585–615.

36. Combrinck JM, Mabotha TE, Ncokazi KK, Ambele MA, Taylor D, Smith PJ, Hoppe HC, Egan TJ. 2013. Insights into the role of heme in the mechanism of action of antimalarials. ACS Chem Biol 8:133–137.

37. Davis TME, Hung TY, Sim IK, Karunajeewa HA, Ilett KF. 2005. Piperaquine. Drugs 65:75–87.

38. O'Neill PM, Barton VE, Ward SA. 2010. The molecular mechanism of action of artemisinin – the debate continues. Molecules 15:1705–1721.

39. Cravo P, Napolitano H, Culleton R. 2015. How genomics is contributing to the fight against artemisinin-resistant malaria parasites. Acta Trop 148:1–7.

40. Machado SG, Robinson GA. 1994. A direct, general approach based on isobolograms for assessing the joint action of drugs in pre-clinical experiments. Stat Med 13:2289–2309.

41. Carter WH, Gennings C, Staniswalis JG, Campbell ED, White KL. 1988. A statistical approach to the construction and analysis of isobolograms. J Am Coll Toxicol 7:963–973.

42. Gennings C. 2000. On testing for drug/chemical interactions: definitions and inference. J Biopharm Stat 10:457–467.

43. Plummer JL, Short TG. 1990. Statistical modeling of the effects of drug combinations. J Pharmacol Methods 23:297–309.

44. Berenbaum MC. 1985. The expected effect of a combination of agents: the general solution. J Theor Biol 114:413–431.

45. McKay MD, Beckman RJ, Conover WJ. 1979. Comparison of three methods for selecting values of input variables in the analysis of output from a computer code. Technometrics 21:239–245.

46. Simpson JA, Price R, Kuile F, Teja-Isavatharm P, Nosten F, Chongsuphajaisiddhi T, Looareesuwan S, Aarons L, White NJ. Population pharmacokinetics of mefloquine in patients with acute falciparum malaria. Clin Pharmacol Ther 66:472–484.

47. Kuile FO ter, Nosten F, Luxemburger C, Kyle D, Teja-Isavatharm P, Phaipun L, Price R, Chongsuphajaisiddhi T, White NJ. 1995. Mefloquine treatment of acute falciparum malaria: a prospective study of non-serious adverse effects in 3673 patients. Bull World Health Organ 73:631–42.

48. Drusano GL, D'Argenio DZ, Symonds W, Bilello PA, McDowell J, Sadler B, Bye A, Bilello JA. 1998. Nucleoside analog 1592u89 and human immunodeficiency virus protease inhibitor 141w94 are synergistic *in vitro*. Antimicrob Agents Chemother 42:2153–2159.

49. Tallarida RJ. 2000. Drug synergism and dose-effect data analysis. Chapman & Hall/CRC.

50. White D, Slocum H, Brun Y, Wrzosek C, Greco W. 2003. A new nonlinear mixture response surface paradigm for the study of synergism: a three drug example. Curr Drug Metab 4:399–409.

51. White NJ. 1997. Assessment of the pharmacodynamic properties of antimalarial drugs *in vivo*. Antimicrob Agents Chemother 41:1413–1422.

515 52. Pasay CJ, Rockett R, Sekuloski S, Griffin P, Marquart L, Peatey C, Wang CYT,
516 O'Rourke P, Elliott S, Baker M, Möhrle JJ, McCarthy JS. 2016. Piperaquine
517 monotherapy of drug-susceptible *Plasmodium falciparum* infection results in rapid
518 clearance of parasitemia but is followed by the appearance of gametocytemia. J
519 Infect Dis 214:105–113.

Tables

Table 1: The Kaplan-Meier estimation of the probabilities of cure on day 42 of follow-up in some regions in South-East Asia where DHA-PQ is the first-line treatment for malaria (19).

	Geographical Region				
	Siem Pang	Binh Phuoc	Bu Gia Map	Aoral	Chi Kraeng
Probability of cure	0.92	0.74	0.67	0.48	0.38
Number of patients	60	40	40	53	40
Year	2015	2015	2015	2015	2014
Country	Cambodia	Viet Nam	Viet Nam	Cambodia	Cambodia

Table 2: Parameter values of the pharmacokinetic model.

The mean values are shown along with the between-patient variabilities (presented as % coefficient of variation) in brackets.

	Drug			
PK parameter	DHA (28)	MQ (27)	PQ (29)	Description
k_a $[1/h]$	0.82 (26.5%)	0.29 (26%)	0.717 (168%)	absorption rate
Cl/F $[L/kg/h]$	1.01 (22.4%)	0.03 (33%)	1.38 (42%)	clearance
V/F $[L/kg]$	0.83 (50%)	10.2 (51%)	-	volume of distribution
V_c/F $[L/kg]$	-	-	180.42 (101%)	volume of central compartment
Q/F $[L/kg/h]$	-	-	2.73 (85%)	inter-compartmental clearance
V_p/F $[L/kg]$	-	-	500 (50%)	volume of peripheral compartment

Table 3: Statistical distribution of the initial parasite burden and parameter values of the PD model.

Parameter	Drug	Distribution	Description
N_0		$\log N(25.46, 1.13)$	initial number of parasites
μ_{IPL}		$DU(4, 16)$	mean of initial parasites age distribution (h)
σ_{IPL}		$DU(2, 8)$	standard deviation of initial age distribution (h)
PMF		TRI$(8, 12, 10)$	parasite multiplication factor (/48 h cycle)
E_{max} *	DHA	TRI$(0.49, 0.69, 0.59)$	maximum killing effect
	PQ	TRI$(0.19, 0.50, 0.35)$	
	MQ	TRI$(0.09, 0.43, 0.26)$	
EC_{50} $[ng/mL]$ †	DHA	$U(1.44, 532.05)$	concentration producing $E_{max}/2$ effect
	PQ	$U(11.56, 94.19)$	
	MQ	$U(20.48, 1087.22)$	
γ	DHA	$\log N(1.31, 0.65)$	sigmoidicity of the concentration-effect curves
	PQ	$\log N(1.35, 0.66)$	
	MQ	$\log N(0.97, 0.54)$	
α	PQ-MQ	TRI$(1, 16, 3.3)$	interaction parameter

TRI(l, h, m): triangular distribution with peak at m, lower limit of l and higher limit of h.

$DU(l, h)$: discrete uniform distribution with lower and higher limits l and h, respectively.

$U(l, h)$: continuous uniform distribution with lower and higher limits l and h, respectively.

$\log N(\mu, \sigma)$: log-normal distribution derived from a normal distribution with mean μ and standard deviation σ.

killing windows of the drugs are as follows (17): $W_{\mathrm{D}} = [6\ 44]$, $W_{\mathrm{P}} = [12\ 36]$ and $W_{\mathrm{M}} = [18\ 40]$

* see Supplementary Material 3 for further details

† the lower limit of the distribution of EC_{50} is chosen to be the *in vitro* IC_{50} of free drug, obtained by adjusting for the *in vitro* drug bindings. The higher limit is chosen to be half of the maximum drug concentration of the median of the PK profiles (17).

Figure legends

Figure 1: Model simulation.

a) PK model results; the concentrations of DHA (blue), PQ (red), MQ (black) are depicted. The shaded regions show the area between the 2.5th and 97.5th percentiles of the results generated for 1000 patients. b) PD model results for 100 randomly selected patients; the horizontal line shows the microscopic level of detection of parasites. c) Kaplan-Meier estimation of the probability of survival over 42 days of follow-up.

Figure 2: Resistance manifestations.

Resistance of parasites to drugs, modelled by relevant alterations of the parameters of the model. A concentration-effect profile of susceptible parasites (black) can be right-shifted, *i.e.* EC_{50} increases (red), and/or the maximum killing effect, E_{max}, decreases (blue).

Figure 3: The probability of cure on day 42 of follow-up when EC_{50} of PQ varies over the deciles of [11 94]**.**

(a) Sensitivity and (b) resistance to DHA. Blue: ACT treatment — dosing regimens of PQ and DHA are 18.0 mg/kg and 4.0 mg/kg, respectively, on days 1, 2 and 3. Purple: a single dose of 8.3 mg/kg of MQ is added on day 3. Black: two 8.3 mg/kg doses of MQ on days 2 and 3 are added. Red: three 8.3 mg/kg doses of MQ are added on days 1, 2, 3. The top labels show the geographical regions in South-East Asia (Table 1) that have observed DHA-PQ cure rates equal to the corresponding simulated values. Error bars show the 95% confidence intervals of Kaplan-Meier analysis.

Figure 4: The influence of antagonism between PQ and MQ on the efficacy of the TACT.

(a) Dashed and solid lines represent combined killing effect, E, for $\alpha = 3.3$ and $\alpha = 1$, respectively. (b) The probability of cure on day 42 of follow-up versus the interaction parameter, α, when the resistance level corresponding to Chi Kraeng is considered, *i.e.* $EC_{50,PQ} \in (69, 78]$; resistance to DHA is assumed. Different values of interaction parameter, α, produce synergism ($0 < \alpha < 1$), zero-interaction ($\alpha = 1$) and antagonism ($1 < \alpha < \infty$) in the combined effect of PQ-MQ. The interpretation of the colors is explained in the caption of Fig. 3.

Figure 5: Interaction between PQ and MQ and their combined effect. (a) Isobologram presented in (13) showing an strong antagonistic interaction between PQ and MQ. The dashed and solid lines show the zero-interaction isobole and our fitted curve to the data points (estimated PQ-MQ interaction parameter is $\alpha = 3.3$), respectively. $C^*_M = C_M/EC_{50,M}$ and $C^*_P = C_P/EC_{50,P}$ are the normalised concentrations of MQ and PQ, respectively. (b) Combined effect of PQ and MQ, *i.e.* E_{PM} (the C^*_M and C^*_P axes are log-scaled), when PQ-MQ interaction parameter (α) equals 3.3. The maximum killing effects and sigmoidicity of PQ and MQ are considered equal (*i.e.* $E_{max,P} = E_{max,M} = 0.3$ and $\gamma_P = \gamma_M = 3$) throughout the model fitting to conform with the data provided by Davis et al. (2006) (13).

Figures

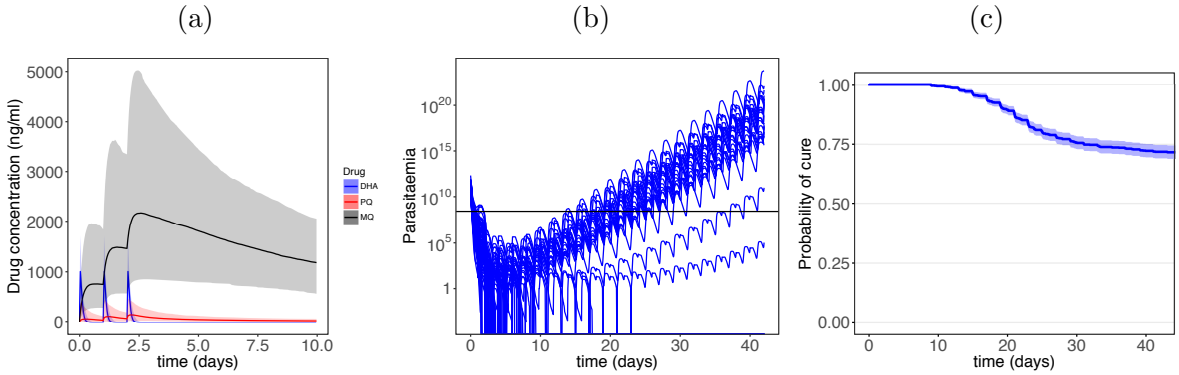

Figure 1

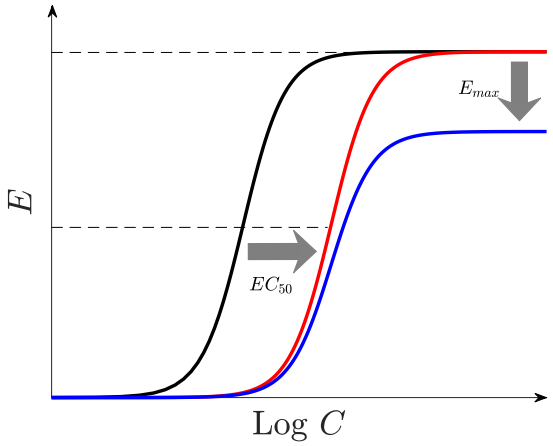

Figure 2

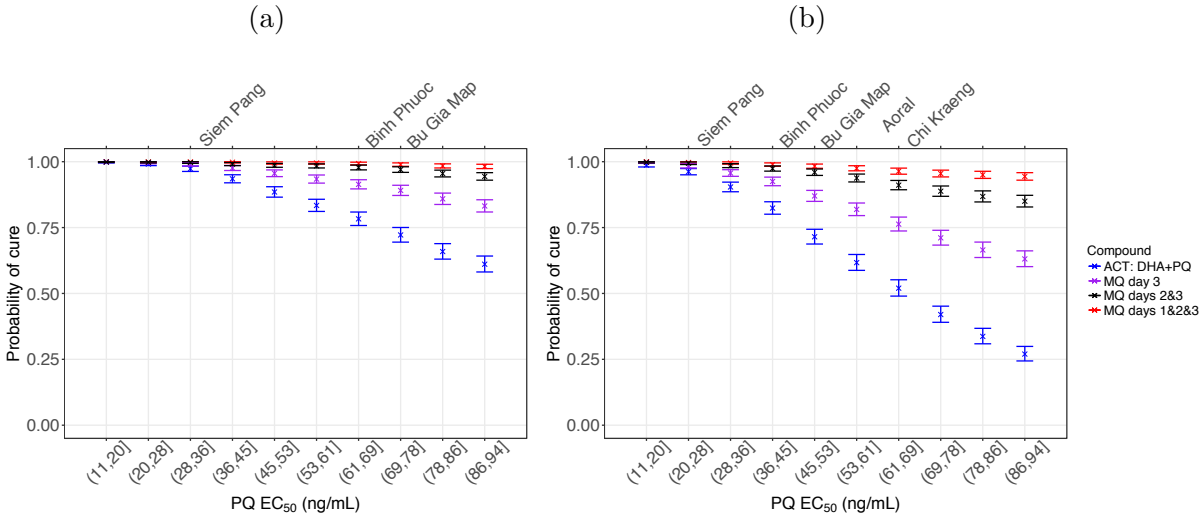

Figure 3

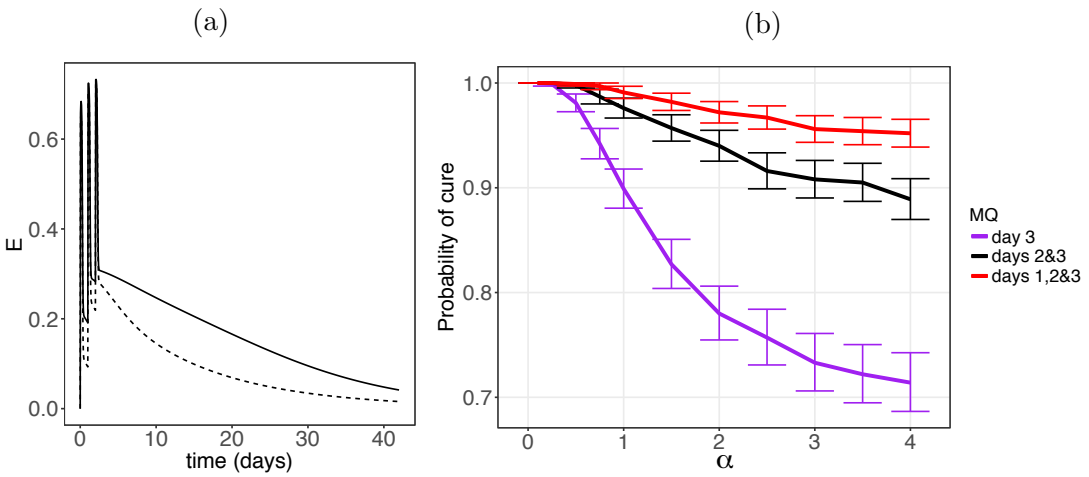

Figure 4

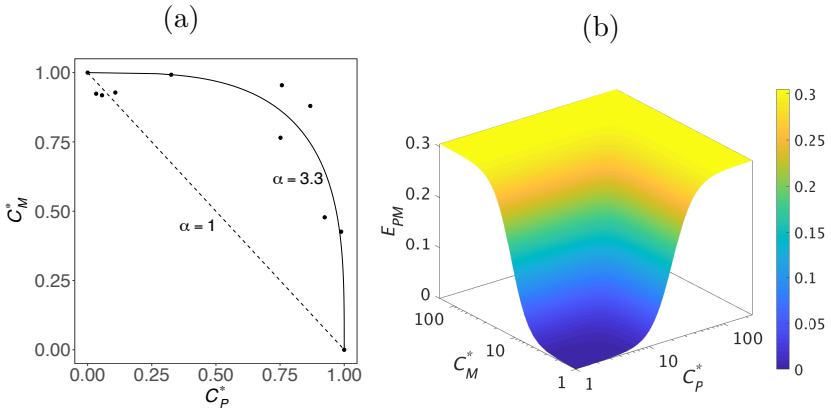

Figure 5

Supplementary Materials

1 Other manifestations of resistance

1.1 Maximum killing effect, E_{max}

Here we examine the probability of cure on day 42 of follow-up when E_{max} is the resistance manifestation. Fig. S1 shows the results when $E_{max,P}$ varies across the deciles of its sampling interval; samples are taken from uniform distributions over each decile. Similar to the results of Section "Resistance to DHA", adding one dose of MQ to the ACT (blue curve) can increase the probability of cure, but is not sufficient. In order to reach the probability of cure of above 90% for all of the deciles, we need three doses of MQ. Of interest, the magnitude of the effect of resistance on probability of cure in this case is close to that of EC_{50}; resistance to DHA is also considered, *i.e.* $EC_{50,D} \in (50, 100]$.

1.2 Killing window, W

We now shorten the size of killing window, W, of PQ for the intra-erythrocytic parasite life cycle, by increasing the lower limit of the W and fixing the higher limit. The results for the ACT show that shortening the killing window can significantly reduce the probability of cure, but again, adding MQ to the compound can pull up the probabilities of cure. To achieve a probability of cure of at least 90%, three 8.3 mg/kg doses of MQ are required.

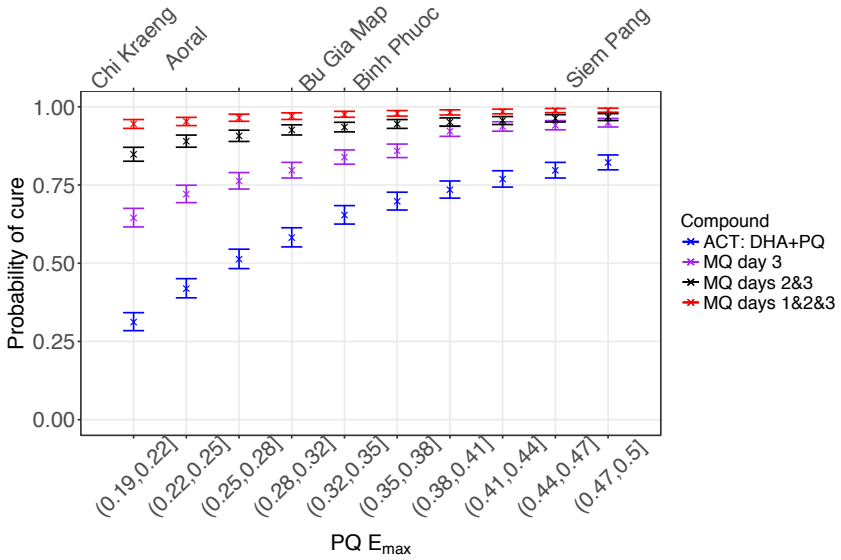

Figure S1: **The probability of cure on day 42 of follow-up when E_{max} of PQ varies over the deciles of** $(0.19, 0.50]$**.**

Dosing regimens of PQ and DHA are 18.0 mg/kg and 4.0 mg/kg, respectively, on days 1, 2 and 3. Purple: a single dose of 8.3 mg/kg of MQ is added on day 3. Black: two 8.3 mg/kg doses of MQ on days 2 and 3 are added. Red: three 8.3 mg/kg doses of MQ are added on days 1, 2, 3. The top labels show the geographical regions in South-East Asia (Table 1) that have observed DHA-PQ cure rates equal to the corresponding simulated values. Error bars show the 95% confidence intervals of Kaplan-Meier analysis.

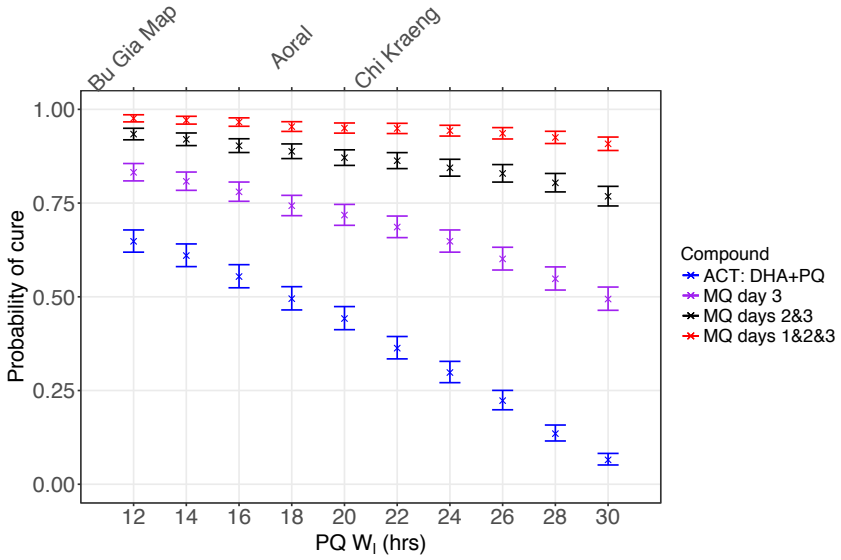

Figure S2: **The probability of cure at day 42 of follow-up when the size of the parasite killing window (W) for PQ is reduced by increasing the lower limit, W_l, from 12 to 30.**

The higher limit, W_u, is constant and equal to 36 hours. Purple: a single dose of 8.3 mg/kg of MQ is added on day 3. Black: two 8.3 mg/kg doses of MQ on days 2 and 3 are added. Red: three 8.3 mg/kg doses of MQ are added on days 1, 2, 3. The top labels show the geographical regions in South-East Asia (Table 1) that have observed DHA-PQ cure rates equal to the corresponding simulated values. Error bars show the 95% confidence intervals of Kaplan-Meier analysis.

2 Modelling combined killing effect

2.1 Models of drug interaction

There are two prominent empirical approaches for modelling zero-interaction: *Loewe additivity* (34) and *Bliss independence* (35). Loewe additivity is based on the idea that two non-interacting drugs differ only in their potency, and was originally formulated as

$$1 = \frac{C_1}{c_1} + \frac{C_2}{c_2}, \tag{2.1}$$

where c_1 and c_2 are the concentrations of drugs 1 and 2, respectively, that each individually (*i.e.* not in combination) produces a specified effect E_{12}, and C_1 and C_2 are the drug concentrations in a combination that together produce E_{12} — for brevity, the formulae are defined for two drugs, but they can be readily extended for multiple drugs. Eqn. (2.1) is known as a *linear isobole*, which is widely used in pharmacology and toxicology as a reference to identify drug interactions. Loewe first put forward this model, which was then investigated more rigorously by Berenbaum (1985) and others.

Loewe additivity is suggested to be a suitable concept for zero-interaction when the combined drugs have similar modes of action (31, 32). However, when the drugs are believed to act independently, Bliss independence is more appropriate. This model is based on a probabilistic perspective, defined as

$$E_{12} = E_1 + E_2 - E_1 E_2 \tag{2.2}$$

where E_1 and E_2 are the individually produced effects by drugs 1 and 2, respectively.

Ultimately, deviations from a selected zero-interaction reference model would determine the degree of synergistic/antagonistic interaction in certain drug combinations. Note that despite the fundamental differences of Loewe additivity and Bliss independence, it has been shown that they indicate the same nature of drug interactions in the majority of cases (48).

2.2 Combined effect of DHA-PQ-MQ

Statistical models can be used to define E_{PM}, *e.g.* Carter et al. (1988) used a generalised linear model with the logit link function:

$$\log\left(\frac{E_{PM}}{1-E_{PM}}\right) = \beta_0 + \beta_1 C_P + \beta_2 C_M + \beta_3 C_P C_M,$$

where C_P and C_M are the concentrations of PQ and MQ, respectively, and $\beta_0, \ldots, \beta_3$ are the coefficients of the model. Similar statistical models can be found in (42, 43).

Another set of models include only one parameter to incorporate the effect of interaction (31, 40, 32). These models are more specified to the framework of drug interaction, in contrast to the statistical models. Here, we focus on the models with one parameter of interaction — noting that statistical models are shown to be readily transformable to these models, *e.g.* see (41).

One of the most frequently used models to describe the combined effect is Greco's

model (31), defined by

$$1 = \frac{C_P}{EC_{50,P}\left(\frac{E_{PM}}{E_{max,P}-E_{PM}}\right)^{\frac{1}{\gamma_P}}} + \frac{C_M}{EC_{50,M}\left(\frac{E_{PM}}{E_{max,M}-E_{PM}}\right)^{\frac{1}{\gamma_M}}} + \frac{\alpha C_P C_M}{EC_{50,P}EC_{50,M}\left(\frac{E_{PM}}{E_{max,P}-E_{PM}}\right)^{\frac{1}{2\gamma_P}}\left(\frac{E_{PM}}{E_{max,M}-E_{PM}}\right)^{\frac{1}{2\gamma_M}}} \tag{2.3}$$

where the subscripts P and M denote which drug the parameters correspond to. The interaction parameter, α, incorporates the influence of the interaction between the drugs, where, for Eqn. (2.3), $\alpha = 0$, $-1 < \alpha < 0$ and $\alpha > 0$ produce zero-interaction, antagonism and synergism, respectively. Note that we should have $E_{PM} < E_{max,P}$ and $E_{PM} < E_{max,M}$, otherwise, Eqn. (2.3) would not yield a real-valued solution for E_{PM}. These conditions thus limit the utility of Greco's model to cases where $E_{max,P} \neq E_{max,M}$.

Tallarida (2006) put forward a broader framework based on the Loewe additivity, from which Greco's model can be derived as a special case. In addition, it overcomes the aforementioned limitation on the values of E_{PM}. In Tallarida's approach, we first identify the more potent drug, say PQ; this can be done by carrying out *in vitro* susceptibility tests or comparing the parasite reduction ratios derived from clinical efficacy studies. Then, we find the concentration of PQ that is equally effective as MQ at concentration C_M, using

$$C_{eq,M} = E_P^{-1}\left(E_M(C_M)\right),$$

where E_P^{-1} is the inverse function of E_P, given by

$$E_P^{-1}(x) = EC_{50,P}\left(\frac{x}{E_{max,P}-x}\right)^{\frac{1}{\gamma_P}},$$

Then, the zero-interaction model is obtained via

$$E_{PM} = E_{max,P}\frac{C_{PM}^{\gamma_P}}{C_{PM}^{\gamma_P} + EC_{50,P}^{\gamma_P}},$$

where

$$C_{PM} = C_P \mathbf{1}_{W_P}(a) + C_{eq,M}\mathbf{1}_{W_M}(a). \tag{2.4}$$

Subsequently, Eqn. (2.4) can be modified to accommodate an interaction between drugs. For example, Tallarida (2000) suggests changing this equation to C_{PM}/α, where α is the interaction parameter. However, we dismiss this method as it does not produce the observed antagonistic isoboles (see Fig. 5), hence, it will not provide a good fit to data. In order to obtain a form of E_{PM} similar to Greco's model, Eqn. (2.3), we then modified Eqn. (2.4) to incorporate the effect of an interaction between drugs. Adding $\alpha C_P C_{eq,M}$ as an extra term to this equation provides a good fit to the data for $\alpha = -0.132$, but, the resultant E_{PM} is non-monotonic, which is biologically infeasible. We also tried other terms such as $\alpha\sqrt{C_P C_{eq,M}}$, but they similarly failed to give either a good fit or a monotonic effect. Hence, the models of form Eqn. (2.3) did not produce an appropriate E_{PM}, as also outlined by White et al. (2003) and Machado, Robinson (1994).

We then turned to using the model introduced by Machado, Robinson (1994):

$$C_{PM} = \left(C_P^{\alpha}\ 1_{W_P}(a) + C_{eq,M}^{\alpha}\ 1_{W_M}(a)\right)^{\frac{1}{\alpha}},$$

where zero-interaction is produced when $\alpha = 1$. The values of $1 < \alpha < \infty$ and $0 < \alpha < 1$ produce antagonism and synergism, respectively. The model provides a good fit to the

data (see Fig. 5a), and importantly, a biologically feasible killing effect, E_{PM} (see Fig. 5b). Therefore, we selected this model for E_{PM}, and used it in the combined effect, Eqn. (1), of the TACT.

To conform with the data provided by Davis et al. (2006) (13), the maximum killing effects and sigmoidicity of PQ and MQ are considered equal (*i.e.* $E_{max,P} = E_{max,M} = 0.3$ and $\gamma_P = \gamma_M = 3$) throughout the model fitting. However, the considered range of variation for α in the simulations is significantly larger than the potential variations due to $E_{max,P} \neq E_{max,M}$ and/or $\gamma_P \neq \gamma_M$, hence, these assumptions do not invalidate the results (see Table 3).

3 Calculating E_{max} using the parasite reduction ratio (PRR)

We are interested in finding how E_{max} is related to the parasite reduction ratio (PRR). We can estimate PRR by

$$PRR = \frac{N_0}{\sum_{a=1}^{48} N(a, t_0 + T)}$$

where T is the time when we count the number of parasites (*e.g.* $T = 48$ hrs) to calculate PRR, and N_0 is the initial number of parasites at time t_0. Then, we have

$$\sum_{a=1}^{48} N(a, t_0) \prod_{\tau=0}^{T-1} (1 - E(a_\tau, t_0 + \tau)) = \frac{N_0}{\text{PMF} \times \text{PRR}},$$

where $a_\tau = [(a + \tau) \bmod 48]$. Thus, we use numerical methods to solve the above equation for E_{max}. The estimated E_{max} values are listed in Table 3. Note that it is extremely important to take account of the details of the clinical efficacy studies, by which the PRRs of the drugs are obtained. We used the following PRRs and the dosing regimens to estimate E_{max} for each drug:

- $\text{PRR}_{DHA} = 10^4$: seven 2 mg/kg doses of DHA are administered (51).
- $\text{PRR}_{PQ} = 2951$: one 14.1 mg/kg dose of PQ is administered (52).
- $\text{PRR}_{MQ} = 100$: one 25 mg/kg dose of MQ is administered (51).

The obtained E_{max} is then used as the median of the triangular distribution (see Table 3), and the lower and higher limits of the distribution are found by

$$E_{max,l} = E_{max} - \frac{\log(50)}{||W||},$$
$$E_{max,h} = E_{max} + \frac{\log(50)}{||W||},$$

where $||W||$ is the size of killing window of the drug (17).